Advances in Chemical Engineering

Chapter 4

Microplasmas and their Application for Nanomaterials Synthesis

***Liang liang Lin*[1,2,*]*; Hongyu Wen*[1]*; Yuan Xia*[2]

[1]*School of Chemical and Material Engineering, Jiangnan University, Wuxi 214122, China.*

[2]*Key Laboratory of Nanodevices of Jiangsu Province, Suzhou 215123, China.*

[*]***Correspondence to: Liang liang Lin,*** *School of Chemical and Material Engineering, Jiangnan University, Wuxi 214122, China.*

Email: linliangliang@jiangnan.edu.cn

Abstract

The pursuit for green, efficient, and controllable synthesis of high quality nanomaterials greatly promotes the development of plasma-assisted nanomaterials synthesis. Owing to their unique characteristics such as atmospheric pressure operation, non-equilibrium chemistry, microcale geometry, and self-organization phenomenon, microplasmas have attracted increasing attention as effective tools for nanofabrication. In this work, nanomaterials and their conventional synthesis methods are briefly introduced, followed by the discussion of typical microplasma systems for nanomaterials synthesis, like gas-phase systems, liquid-involved systems, and microfluidic plasmas. Meanwhile, representative configurations in each system are elaborated to show how nanomaterials are prepared. Afterwards, the diagnostic techniques for analyzing both the microplasma-reaction process as well as the generated nanoparticles are comprehensively reviewed, CCD camera, electrical measurement, optical emission spectrometry, scattering technique, TEM, SEM, EDX, XRD, Raman, XPS, FT-IR, etc. Finally, salient examples are given to show various types of nanomaterials obtained by microplasmas. The motivation of this work is to provide readers essential information of the microplasma technique, which may enlighten them alternative way for functional nanomaterials synthesis and help to guide them in the process design.

Keywords: Plasma Technology; Plasma Nanofabrication; Microplasma; Functional Nanomaterials; Microfluidics.

1. Introduction

1.1. Nanomaterials synthesis

Due to their low dimensions and large surface area, nanomaterials exhibit unique properties, making them attractive for applications like catalysis, bio-sensing [1], drug delivery [2], imaging [3], energy storage [4], biomedicine [5], etc. In the past few decades, a tremendous efforts have been devoted to the manufacturing of nanomaterials with controllable size, shape and structure, aiming to understand how these parameters affect the properties of nanoparticles, and eventually customize them for specific applications. The extensive research has also led to a variety of novel or established methods for nanofabrication, which can be generally classified physical methods, wet-chemistry approaches, and bio-assisted strategies.

Despite significant progress has been achieved in preparing nanomaterials with tunable properties, limitations still exist. For instance, physical methods commonly need time/energy-consuming procedures and inert atmospheres, requiring a lot of equipment and operating costs. For wet-chemistry methods, an inevitable problem is the introduction or production of by-products (for example, surfactants, reducing agents and stabilizers), and requiring subsequent purification steps after synthesis. In some cases, post-treatment such as calcination or annealing is necessitated to improve the crystallinity of the product. As to the bio-assisted processes, they are relatively complex, and the properties of the products are difficult to control and adjust. Furthermore, since the source of plant/microorganism is independent and has a considerable influence on the nanoparticles, the uniformity of the product is low in industrial application. Therefore, by state-of-art techniques, it is still challenging to synthesize nanomaterials with desired properties in a simple, environmentally friendly and efficient way.

1.2. Plasma technology and plasma nanofabrication

Plasma is considered to be the fourth state of materials, containing reactive species such as electrons, ions, neutral atom, molecules and metastable radicals. In general, plasmas are divided into two categories: thermal (equilibrium) plasmas and non-thermal (non-equilibrium) plasmas. In thermal plasmas, due to the rather short mean free path of particles as well as high collision frequency, all species have the same temperature (~103-104 K). By contrast, in non-thermal plasmas, electrons gain energies in the range of ~eV from the electric field to maintain the ionization balance, and are thus the hottest species in plasmas, while heavy particles such as neutral species and ions are at a temperature of a few hundred K or lower. The selective heating of electrons by electric fields leaves the heavy particles (ions, neutral species) cold. Moreover, the collision frequency of electrons is typically 2-3 orders of magnitude larger than that of heavy particles. The energetic electrons further generate high densities of excited

species or radicals (metastable species) through inelastic electron-impact excitation and dissociation collisions, helping to accelerate chemical reactions and bring the processes into the otherwise hard to achieve parameter spaces. **(Table 1)** lists typical temperatures and speeds of the selected species in non-thermal plasmas.

Table 1: Typical temperatures and speeds of non-thermal plasma species.

Species	Typical temperature (eV)	Typical temperature (K)	Typical speed (m/s)
e	1~5	11000~55000	6.6×10^5~1.5×10^6
Ar^+	0.025~0.1	300~1200	400~800
He^+	0.025~0.1	300~1200	1200~2400

With the development of plasma technology, now it has covered various fields ranging from ozone generation, light source, thin film deposition and etching, to VOC decomposition, CO2 conversion, surface functionalization, medical treatment, and so on. In addition, driven by its fascinating properties, synthesis of plasma-assisted nanomaterials has also attracted a great attention. In plasma enhanced chemistry, charged particles, excited states and free radicals are expected to play a role in nanofabrication, which is essentially different from traditional solution-based media. Electrons in plasma have sufficient energy to trigger plasma chemical reactions through collisions with precursor compounds [6]. Therefore, these processes are essentially solvent-free and ligand-free [7]. In some cases, due to the high-energy species, plasma-based methods provide a highly reactive condition for the nucleation of atoms, enabling reactions that are hardly achievable in a mild way [8]. In addition, high concentrations of low-energy electrons help to enhance plasma chemistry caused by vibrational excitation, thus reducing the cost of energy production [9].

Over the past few decades, a series of plasma-based technical platforms and methods have been developed. Various kinds of nanomaterials were synthesized under different conditions, such as carbide nanoparticles, nitride powders, oxide nanomaterials, metal nanoparticles or alloys, polymers, etc. Although great progress has been made in the manufacture of plasma-assisted nanomaterials in the past few years, there still several challenges need to be addressed. At present, most of the reported processes operate at low pressure and require expensive vacuum equipment, which makes industrial application impractical. Besides, the microcosmic and macroscopic parameters related to the process in plasma, such as electron density, electron energy, temperature, current density and weakening electric field, often have uneven spatial distribution, so it is difficult to provide uniform conditions for the nucleation and growth of particles. Therefore, the products usually have the characteristics of wide particle size distribution and partial agglomeration [10, 11]. In order to obtain the parameters of microplasma, it is necessary to combine plasma production and diagnostic experiments, supplemented by numerical simulation. **(Table 2)** lists typical parameters of various types of microplasmas.

Table 2: Typical parameters of various types of microplasmas.

	Microwave-based [12]	RF needle [13-15]	RF jet [16]	VHF jet [17]	MW microgap [18]	DC hollow cathode [19]	Pulsed DC microgap [20]
Frequency	2.45 GHz	13.56 MHz	13.56 MHz	100 MHz	2.45 GHz	N/A	10 kHz
Working gases	Ar, Ar/C_2H_2, N_2	He, He/N_2	Ar, He, Ar/CH_4, Ar/C_2H_2	Ar, Ar/SF_6	air, He/N_2(5%)	Ar	Ar
Absorbed power [W]	(5-15) for Ar 100 for N_2 40 for Ar/C_2H_2	(0.01-10)	(15-30)	200	100[21]	12	~6
Gas temperature [K]	from 303 in Ar [22, 23]	from 310 in He				700-1800	
OES temperatures [K]	rotational: 2700 in N_2, [N_2 (2+)] 6500 in N_2, [N_2^+ (1-)] 4500 in N_2, (CN violet) 3500 in C_2H_2, (C_2 Swan)	rotational: 300-700 in He/N_2 [N_2 (2+)]	rotational: 300-350 in He (OH) 300 in Ar (OH)	rotational: 5000-6000 (Ar atoms)	rotational: 2500 in air [N_2 (2+)] 1200 in He/N_2(5%) [N_2 (2+)]	electron temperature: 1 eV by Boltzmann plot	electron temperature: 0.9±0.3 eV in Ar
Electron densities [cm^{-3}]	6×10^{14}–1.4×10^{15} in Ar (H_β)	4×10^{10}–8×10^{10} in He (estimation)	8.5×10^{14} in Ar 7×10^{14} in He (H_β)	2×10^{14}-1.3×10^{15} in Ar (H_β)	1.8×10^{15} in air 3×10^{14} in He/N_2(5%)	10^{15} cm^3 in Ar	$(6\pm3)\times10^{13}$ cm^3 in Ar

1.3. Microplasma-assisted nanomaterials synthesis

As a special category of plasma being confined within submillimeter scale in at least one dimension, microplasma has attracted tremendous interests for nanofabrication due to their unique characteristics. In general, it employs beneficial properties of the atmospheric pressure gas discharge in microscale geometry for various plasma-enabled processes, resulting in a new and facile branch of applied plasma science. Several key advantages of microplasma-assited nanofabrication were summarized by Mariotti D and RM Sankaran: high pressure chemistry, continuous-flow, microreactor geometry and self-assembly/organization (Mariotti D and RM Sankaran, 2010). From a cost efficiency standpoint, the atmospheric pressure operation of microplasmas allows saving of the significant costs associated with maintaining vacuum and using complex transfer chambers. From the process efficiency perspective, microplasmas are characterized by higher densities of radicals, resulting in higher rates of plasma-chemical reactions and, in case of nanomaterials synthesis, leading to improved efficiency in particle nucleation and growth. Meanwhile, since the micro-scale geometry ensures a short residence time with a narrow residence time distribution (RTD) for precursors, the obtained nanoparticles are relatively smaller and have narrower size distributions compared with bulk plasma

processes. In addition, the safety risks are much reduced when operating in micro-scale, especially when handling toxic materials. Based on these reasons, microplasma is becoming an emerging technique for nanofabrication, and a growing number of researches have been carried out in recent years focusing on its application in metallic nanoparticles synthesis.

This chapter mainly focuses on the state of art of functional nanomaterials synthesized by microplasmas, which covers the discussion of typical microplasma systems, the commonly used diagnostic techniques in microplasma nanofabrication processes, the nanomaterials obtained by microplamas, etc. Hopefully this chapter can introduce this novel technique as well as the essential information to readers.

2. Representative Microplasma Configurations for Nanomaterials Synthesis

So far, a wide range of microplasma systems have been developed for nano-manufacturing. It is classified according to plasma power source (excitation frequency), electrode geometry, power coupling method, precursor injection mode, target product and so on. According to the general configuration of microplasma system for the synthesis of nanomaterials, it can be divided into three categories: gas-phase systems, liquid-involved systems, and microfluidic plasma systems.

2.1. Gas-phase systems

2.1.1. Hollow electrode micro-discharge

The micro-discharge of hollow electrode is a relatively simple structure for the preparation of nanomaterials, which can operate stably at atmospheric pressure and room temperature. Generally, there are two metal hollow capillaries separated by 1~2 mm, both of which are connected to DC power supply and are used as cathodes and anodes respectively. At the same time, they are also used as precursor transporters, which are introduced by inert gases such as argon and helium and separated in the plasma zone between the two electrodes. The formed aerosol particles can be collected by an electrostatic precipitator or a filter installed at the back of the reactor. In a typical micro-charge of hollow electrode, the typical voltage and current used to prepare nanomaterials are at the level of several hundred V and several mA, their energy is too small to ionize the electrode. Therefore, the electrode will not participate in the reaction.

A representative configuration demonstrated by PA Lin et al. is shown in (**Figure 1)** [24], in which various organometallic compounds (nickelocene, ferrocene, copper acetylacetonate and platinum acetylacetonate) were employed to produce metallic nanoparticles and multi-metallic nanoparticles. In this research two SS capillary tubes (O.D.=1.6 mm, I.D.=180 μm) were used as the cathode and the anode. After subliming the corresponding metallic

precursors, they were carried into the plasma zone by the separate gas lines in continuous argon flows. In all experiments the total gas flow was kept constant at 100 sccm, and the gas flow rates in different precursors lines were individually controlled by mass flow controllers. In this manner metallic nano-alloys of tunable composition were produced by varying the relative gas flow rate in precursor and dilution gas lines. The size and size distributions of the generated nanoparticles were measured in situ by a scanning mobility particle sizing system. In addition to the preparation of metal nanoparticles and carbon nanotubes, hollow electrode micro-discharges are also used to prepare silicon nanowires or nanodiamonds [25]. Results show that this method can prepare ultra-fine nanoparticles at atmospheric pressure and room temperature.

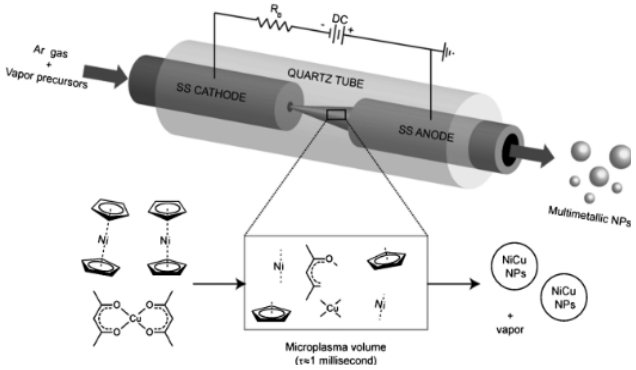

Figure 1: Schematic diagram of the atmospheric pressure microplasma reactor used to continuously synthesize compositionally tunable multimetallic nanoparticles (NPs). A hypothesized mechanism for formation of Ni_xCu_{1-x} bimetallic NPs is also shown.

2.1.2. Microplasma jets

At present, various configurations of microplasma jets have been proposed and used as tools for the manufacture of nanomaterials, using different types of power supplies (DC, RF or microwave) to ignite and maintain plasma. Gas jets and external electrodes, such as wire electrodes or tube electrodes, are established. Belmonte et al. [10] pointed out that with regard to the microplasma jet, the following three problems need to be solved: (1) the location of the deposition region is controlled by adjusting the flow rate of the precursor-the most commonly used method is to locate the capillaries through which the precursor flows. (2) Management of consumable wires for nanomaterial sources - most microplasma jets use expendable wires as precursors of the nanostructures to be built; the wires are consumed as the reaction progresses. (3) The power supply (DC, RF or microwave) is coupled to the system to form plasma. the power supply has a great influence on the growth of nanomaterials, and different methods are adopted according to different settings. According to whether consumable wires are used as electrodes, microplasma jets can be divided into two types.

a. Consumable electrode microplasma jet

In many microplasma jets, consumable wires are used as precursors. Therefore, metal wires such as W [26, 27], Fe [26], Cu [26], Mo [28, 29] and Au [30] are reported to be used

to prepare required nanomaterials. Generally speaking, the structure of microplasma jet with consumable wire as electrode is very similar. Metal wires are usually used as solid precursors and inserted into capillaries. Various plasma gases such as Ar, He, N2, H2, O2 or their mixtures form plasmas through capillaries. According to the different coupling mode of power supply, microplasma can be formed inside or outside the tube. Part of the wire is located in the microplasma, and its surface will react. In this configuration, different nanomaterial structures can be obtained on the surface of the wire or on the substrate below the plasma jet [31]. In the process of deposition, a wide range of nanomaterials can be produced by changing the process parameters such as gas flow rate, gas composition, substrate distance and input power. The results show that, compared with other methods, this method is a cost-effective and widely used method for the preparation of metal/metal oxide nanomaterials.

A typical example of the microplasma jet with a consuming electrode is shown in **(Figure 2)** (Y Shimizu et al., 2006). In this structure an argon flow of 30 sccm flow rate was injected into a quartz capillary (O.D.= 1.0 mm, I.D.=300-700 μm). A pinched nozzle covered with a quartz tube (O.D.= 1.5 mm, I.D.=1.1 mm) was used to prevent breakdown due to its susceptibility to mechanical shock. Consumable metal wires such as tungsten, iron, or copper were inserted into the nozzle as the electrode, while the other end of the wire was affixed to the inner wall of the metal tube. The nozzle was connected to the argon line for plasma-gas introduction via a metal tube. Once the microplasma jet was ignited, the wires were melted or evaporated efficiently by inductive heating as well as heat conduction from the microplasma. The resulting atomized droplets were jetted out with plasma-gas flowing, and were oxidized during the processing to deposit metal oxide grains on polymeric substrates. It is demonstrated that Fe and Cu wires are consumed to form their oxide dots on glass epoxy substrates, and tower-shaped deposits with a deposition rate of 50μm/s can be achieved. Because of the low heat flux due to small plasma size and low energy supply, this spraying is useful for deposition on low melting-point polymeric substrates.

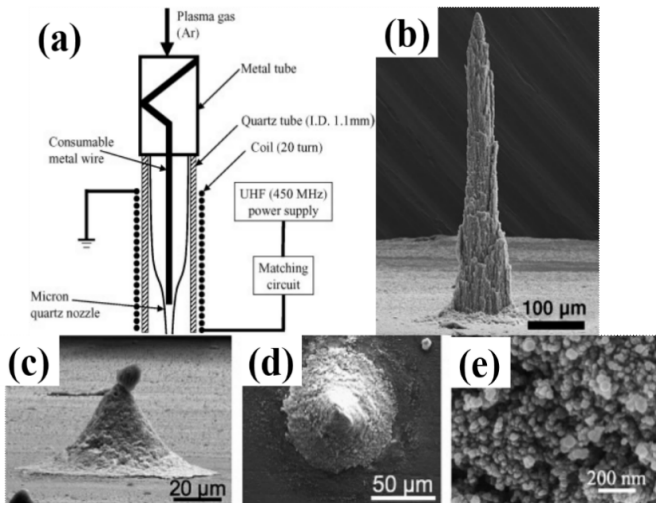

Figure 2: Schematic diagram of the microplasma jet with consumable metal wires to synthesize metal oxides nanoparticles.

b. External electrode microplasma jets

There are also reports of using tubes or external electrodes to replace consumable wires to form plasma jets. In this case, additional precursors, such as CH4 [32, 33], SiCl4 [33], Ti[OC3H7]4 [34], Pd(hfac)2 [35] and Cu(hfac)2 [35], are provided to prepare the desired product. Compared with the microplasma using consumable wires as electrodes, this type of microplasma jet has no direct interaction between plasma and electrode materials, thus eliminating possible contaminations. Meanwhile, the process has larger operational space, since a wider range of processing parameters can be set and tuned, such as precursor's ratio, the power coupling mode, the applied voltage frequency, precursor residence time and so on. In terms of precursors, this type of plasma has more flexibility. Due to the possibility to confine the plasma jet either partially or totally within the tube, in principle, metallic precursors can be gases, liquids or even solids, as long as the jet is appropriately positioned.

A typical example of microplasma jets with external electrodes is illustrated in (**Figure 3)**, where a plasma jet was totally confined inside a DBD reactor to produce Ni nanoparticles from nickelocene vapors 76. In this study, two types of DBD reactor, with or without a gas injection capillary, were applied in order to control and study the particle nucleation and growth. Both reactors consisted of a quartz tube (O.D.= 6 mm, I.D.=2 mm) with powered electrodes outside the quartz tube. The plasmas were ignited and operated at steady state by an AC power supply. Copper tapes with the width of 3-4 mm were wrapped around the exterior of the quartz tubes and operated as the powered electrodes. The discharge was sustained at the frequency of 20-30 kHz with peak-to-peak voltage of ~8 kV, being measured by a high voltage probe. Nickelocene vapors of different concentrations (0.21-0.94 ppm) were carried into the plasma zone by an argon flow of 100 sccm flow rate. The generated nanoparticles were collected by a 40 μm pore size Teflon filter placed at the gas effluent of the reactor.

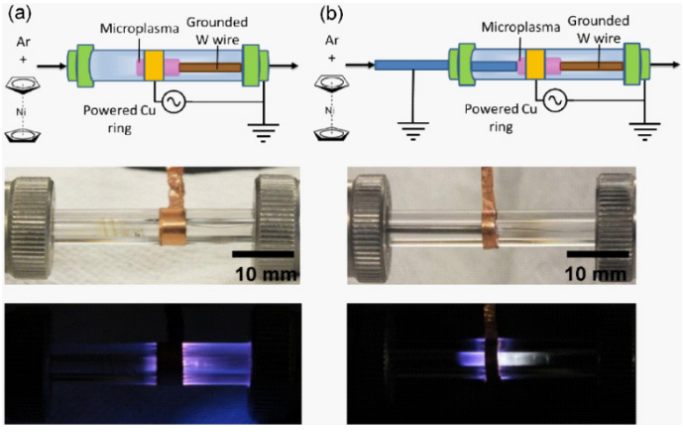

Figure 3: Schematic illustration and photos of a totally confined microplasma jet (DBD) with external electrodes: (a) without and (b) with a capillary gas injection for Ni nanofabrication [36].

Na Lu et al. investigated the CO2 conversion promoted by γ-Al2O3 supported potassium intercalated g-C3N4 (KuCN/ AO) catalyst in a packed-bed dielectric barrier discharge (DBD) plasma system. A coaxial cylinder DBD plasma reactor was used with Cu powder as the high

voltage electrode **(Figure 4).** Reactor temperature showed converse effect on CO2 conversion. As the reactor temperature decreased from 120 ℃ to 50 ℃, CO2 conversion rate and energy efficiency both increased 50%. They found that after the catalyst was filled into the discharge area, the discharge mode changed from filamentary discharge to the combination of filamentary-surface discharge. In this work, synergistic effect of DBD plasma using copper powder as high voltage electrode and K intercalated g-C3N4 (KuCN) catalyst in CO2 conversion was proposed for the first time, and is expected to be significance for promoting the application of plasma-catalytic technology in CO2 conversion. Meanwhile KuCN catalyst was prepared with KBr and urea as precursors. The γ-Al2O3 spheres loaded with KuCN catalyst (KuCN/AO) were filled in the gap of coaxial cylinder reactor to construct packed-bed DBD discharge plasma system for the investigation of CO2 conversion [37].

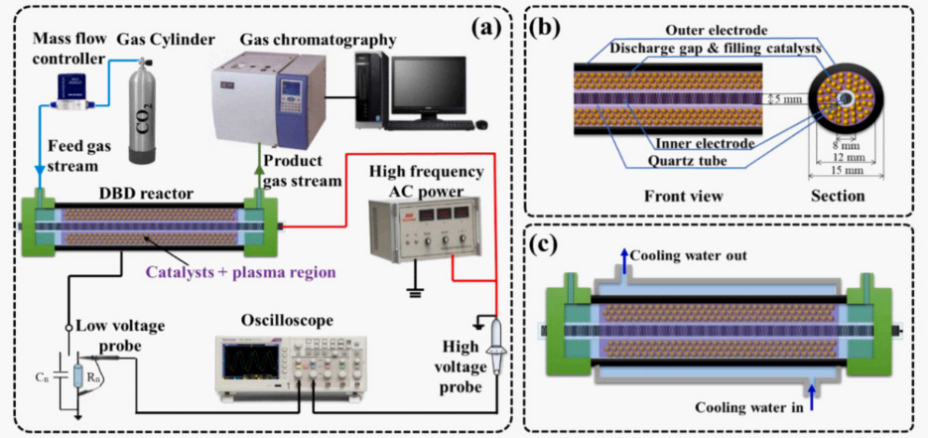

Figure 4: (a) the schematic diagram of the experimental system; (b) the detailed structure of the coaxial cylindrical DBD reactor; (c) The schematic diagram of the cooling device.

2.2. Liquid-involved systems

Except the formation of microplasma in the gas phase, researchers have also developed a series of methods to generate microplasma through liquid device, such as DC power supply, high-frequency power supply, pulse high-voltage power supply and several other methods. Plasma-liquid interaction is a multidisciplinary topic including physics, chemistry, electrical and materials science being fundamentally different from classical systems with solid electrodes and liquid electrolytes. In past decades, with the development of nanoscience and the emergence of various reactors based on plasma-liquid interaction, an important question was naturally raised: Can charged radicals be transferred between plasmas and electrolytes to enable chemical or electrochemical reactions and to produce nanoparticles of controlled properties in the plasma-liquid systems? The pursuit of the answer to this question attracted significant academic research from different fields, and many studies were carried to investigate fascinating interfacial phenomena.

Liquid-phase microplasma configurations is a novel method to produce nanoparticles in aqueous solution. It is known that the density of liquids is much higher than that of gases. Compared with the gas phase plasma, moving the plasma to the liquid phase makes the pressure

increase more significantly, resulting in additional restrictions on the plasma [38]. This highly restricted partial discharge provides a potential way for the direct and efficient preparation of nanomaterials. In addition, many active chemicals, including OH•, O•, H•, H2O2 and O3, which can be formed in the aqueous phase and beneficial to nano-crystallization. Some studies have also shown that water may contribute to the non-equilibrium state of microplasma. It is well known that a small part of the energy coupled with electrons in a plasma can heat a gas. In the liquid plasma, water as a radiator, heat could be lost quickly, thus preventing the gas temperature from rising sharply and keeping the non-equilibrium state [39].

Liquid phase micro-plasma devices can be divided into two types: non-contact glow charge electrolysis (GDE) and contact glow charge electrolysis (CGDE) [40]. The former forms plasma in the gas phase above the surface of the solution, while the latter forms plasma in the interior of the solution. In a word, the interface between plasma and liquid is a highly complex region, and there are many kinds of phases (gas, liquid and vapor). In addition, charged or highly active substances such as gas ions and solution ions, electrons and free radicals make liquid-phase microplasmas have broad application prospects in various fields. One of the particularly interesting applications is the synthesis of nanomaterials [41].

2.2.1. Non-contact glow charge electrolysis (GDE)

Non-contact plasma-liquid systems refer to the configurations where plasmas are formed in the gas phase above the solution surface. Usually one electrode is in the form of “pin” or with a sharp “edge” and put in the gas phase within a distance of 2 mm above the liquid electrolyte, while the other electrode is immersed inside the electrolyte and can be in various shapes. Power supplies of different frequencies ranging from dc, kHz, MHz and even to GHz are coupled on the electrodes to excite and sustain the plasma [39]. In this sense the discharge is generated between the upper electrode and the electrolyte surface, and the metallic precursors dissolved in the electrolyte will be reduced to form metallic nanoparticles by electrons under the plasma treatment. With few exceptions which involving ionic liquids, such plasma systems are operated at atmospheric pressure or higher [42, 43].

A typical example of the indirect contact plasma-liquid system is shown in Fig. 5(a-b), where the HAuCl4 solution (0.2 mM) was used as the electrolyte to produce gold nanoparticles [44]. In this research a SS capillary tube (I.D.= 175 μm, Length= 5 cm) was used as the cathode and positioned 2 mm above the electrolyte surface. A Pt foil (Area= 1 × 1 cm2, thickness= 0.001 inch) functioned as the anode and was placed 3 cm away from the cathode. Both electrodes were connected to a DC high voltage power supply, and plasma was formed between the capillary tube and the electrolyte surface. For each operation a helium flow of 25 sccm gas flow rate was coupled to the capillary acting as the plasma gas. A 10 ml solution of HAuCl4 was put in a petri dish, with a 0.01 M fructose added to prevent uncontrolled particle

growth and agglomeration. Meanwhile, processing parameters such as solution temperature, current, and rate of stirring could be adjusted to synthesize Au nanoparticles of controllable size and morphology. In addition to metal nanoparticles, same method was also applied for the synthesis of nanoalloys. As reported by Ostrikov et al., AuxAg1-x nanoparticles with tunable plasmonic responses were successfully fabricated by the microplasma process. The size and the composition of the AuxAg1-x NPs can be effectively controlled by variation of the reaction time **(Figure 5(c-g))**.

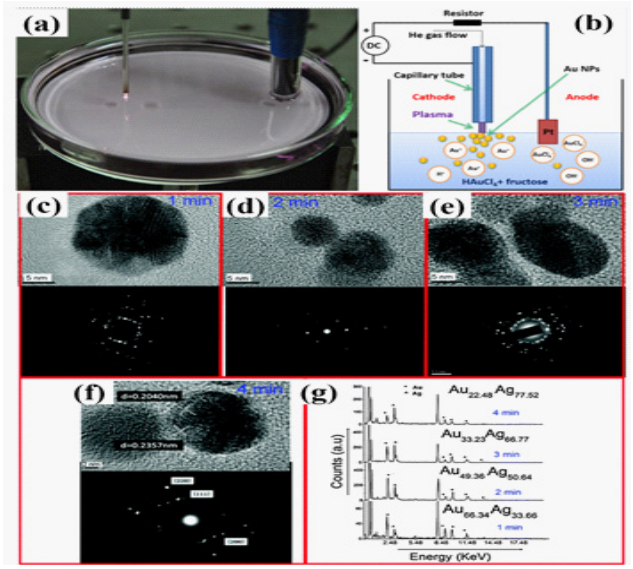

Figure 5: (a-b) The experiment setup of the indirect contact plasma-liquid system for preparing Au nanoparticles; (c-g) same method was extend to the synthesis of AuxAg1-x nanoalloys.

Instead of using aqueous solution of metal salts, there are also using ionic liquids as the electrolyte, since ionic liquids have unique physicochemical properties such as high thermal stability, excellent ionic conductivity, low viscosity and extremely low vapor pressures [45-47]. Besides, another distinctive advantage is their wide electrochemical windows (up to 7 Volt), enabling them to electrodeposit elements such as Ge, Si, Se, Al and many others that cannot be obtained in aqueous solutions [43].

In the study of SA Meiss et al. [43], they used a solution of AgCF3SO3 and 1-butyl-3-methylimidazolium trifluoromethylsulfonate ionic liquid ([BMIm] [TfO]) as the electrolyte for the liquid phase synthesis of Ag nanoparticles in a glass tube (I.D.= 2.5 cm). The solution typically contained 0.3 g of AgCF3SO3 in 10 mL ([BMIm] [TfO]). The anode was a platinum sheet (1 cm×1 cm) and immersed inside the ionic liquid, while the cathode was a platinum hollow cylinder (Diameter= 0.75 cm, Length= 1.5 cm) and placed in the gas phase above the ionic liquid. The reactor was evacuated before each operation, and the pressure was controlled at 1 mbar in an argon atmosphere. During the experiment the current was set at 10 mA, and the voltage stabilized at about 470 V. Results showed black reaction products were formed at the plasma-ionic liquid surface after several minutes, which were dispersed and later deposited at the bottom of reactor **(Figure 6).** Further characterization indicated they were consisted of crystalline Ag nanoparticles with a main distribution in the range of 8-30 nm.

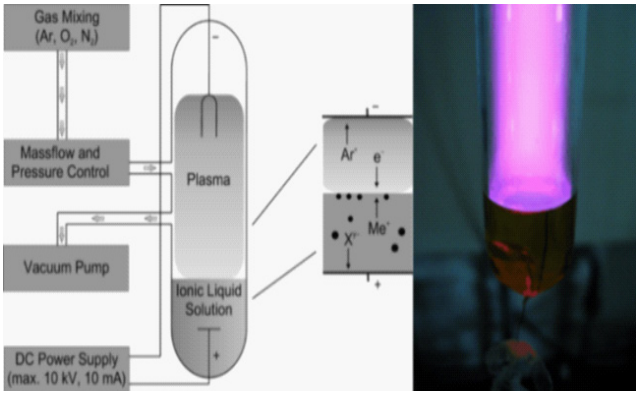

Figure 6: The indirect contact plasma-liquid system using ionic liquid as the electrolyte to prepare silver nanoparticles.

2.2.2. Contact glow charge electrolysis (CGDE)

Contact plasma-liquid systems refer to the configurations where plasmas are generated within the liquid instead of in the gas phase above the liquid. Generally the plasma gas is not necessitated, but a large quantity of heat and a high yield of solvent-split radicals are generated in the solution. The precursor can be either metallic salts that being dissolved in the water or other solvents to form the electrolyte, or metal wires functioning as the consuming electrodes. Moreover, due to the pressure originating from the liquid, plasma usually operates at pressures a slightly higher than atmospheric pressure. In light of the configuration, the electrodes are mostly in the form of pin-to-pin or pin-to-plate structure, with a characteristic distance of ~mm. The discharges are commonly produced by high voltage pulses and referred as streamers or corona discharges. A common excitation method is by means of discharging a capacitor where a short-rise-time switch (e.g. a spark gap) produces microsecond pulsed discharges. Recently, more excitation methods are applied to generate the plasma in the liquid phase, like nanosecond pulses, radio frequency powers or microwave plasmas.

One representative example is demonstrated in **(Figure 7)**, where Sn nanoparticles were successfully synthesized by a direct contact plasma-liquid system. In this study the tin chloride dehydrate (SnCl2·2H2O) was used as the precursor for the Sn nanoparticles, and the cetyltrimethylammonium bromide (CTAB, CH3(CH2)15N(CH3)3Br) was used as the surfactant. Both were dissolved in pure water to prepare the electrolyte. During each operation a 300 ml electrolyte with tin chloride concentration of 2-4 mM was added in the reactor. Tungsten capillaries (Diameter= 2 mm) coated by ceramic insulator were chosen as the electrodes and fixed in the “needle-to-needle” form, with an electrode gap of 0.2 mm. A high-frequency bipolar pulse power supply was applied to generate the plasmas directly in the liquid phase in a double annular tube type reactor (I.D.= 50 mm, O.D.= 80 mm, Height= 150 mm), and the applied voltage, pulse width and frequency were fixed at 250 V, 5 μs and 30 kHz, respectively. Under the plasma treatment the Sn2+ was reduced to form the Sn nanoparticles.

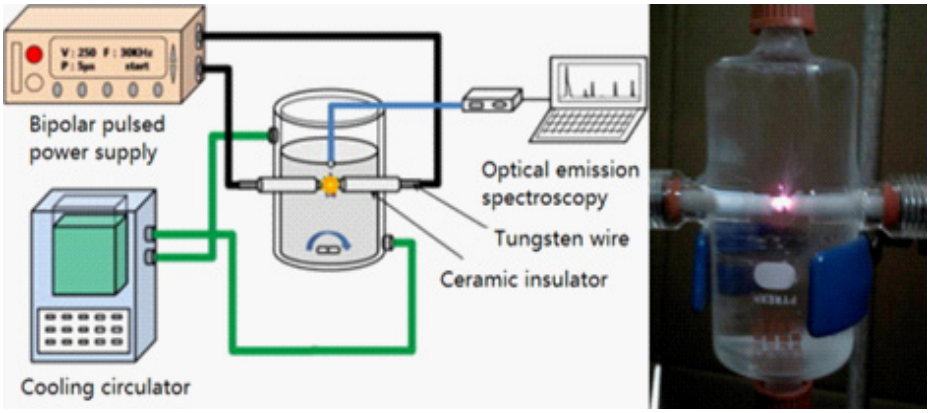

Figure 7: The schematic setup and the photograph of the direct contact plasma-liquid system for the synthesis of Sn nanoparticles [48, 49].

It is generally believed that liquid microplasma will provide potential guidance for a variety of applications, such as nanoparticle synthesis [50], flame electrochemistry [51], spectrochemical analysis, wastewater remediation [52] and so on. However, the underlying mechanism of the reaction is still unclear, and the chemical and electrochemical processes are still unclear. At present, there are only several kinds of nanoparticles prepared by this method, such as Au [53], Fe3O4 [54], Cu2O [55], Ag [41, 56], Cu [57] and Ti [58]. In some ways, the current state of liquid microplasma is still regarded as an "art" rather than an "exact science" [40], and more research is needed to solve these puzzles.

In summary, we have shown representative examples of each microplasma configuration for nanoparticle synthesis both in gas phase and the liquid phase. In order to provide a guideline for the process design and for the selection of an appropriate microplasma system for nanoparticles synthesis, a brief summary of the advantages and drawbacks of each configuration is provided in **(Table 3).**

Table 3: A summary of advantages and drawbacks of the microplasma systems for nanoparticles synthesis.

Plasma configurations	Advantages	Drawbacks
Hollow-electrode microdischarges	Simple, safe, easy operation Low power consumption Ultra-fine particle size, narrow size distribution	Extremely low throughput Metal contaminations Unstable conditions after long time operation
Microplasma jets with external electrodes	Efficient, flexible, high purity products Wide operational windows Flexible precursors (gas, liquid and solid) In-situ deposition, i.e. printing, coating	Large particle size, broad size distribution Expensive and complex power supply
Microplasma jets with consuming electrodes	Simple, efficient, flexible, in-flight tuning A series of metallic nanoparticles Feasible for oxides, alloys, nitrides	Batch process due to metal wires consumption Large particle size, broad size distribution
Liquid-involved systems	Flexible, efficient, simple and highly confined High radical density, low temperature Ultra-fine particle size, narrow size distribution Flexible precursors (salts, consuming wires)	Post-treatment required Batch process due to solvent evaporation Complex process, unclear mechanisms

2.3. Microfluidic plasmas

2.3.1. Integration of plasma with microfluidics

Microfluidic is the basic principle of microreactor technology [59]. The latter makes flow chemistry [60] and the use of new process controls possible [61], an unconventional chemical mode of operation with great destructive potential that enhances sustainability [62]. In commercial applications, this approach is often referred to as continuous flow processing [62], which means making a compromise when moving from a favorable microscopic level to a more practical millisecond level; it refers to the characteristic size that determines the performance of the reactor. Continuous manufacturing technology produces products without ceasing. In contrast, mass production technology manufactures products in the form of charge-wise pattern, with start-up and shutdown procedures. Henry Ford's automated assembly line is a key example of continuous production. A car is built step by step in time and space continuously. Continuous flow is particularly effective on a small scale, that is, the so-called microfluidic [63]. Mass and heat transfer are maximized, making it possible to improve the best performance of chemical products. Continuous flow has many other advantages, such as periodic flow mode, (inherent) security, high product quality, compact integration opportunities, and so on. See literature review [59, 60, 64].

For the generation of microfluidic plasmas, one should provide a certain energy to the microfluidic system to generate the plasma particles (e.g., energetic electrons and ions, excited atoms, molecules, radicals, photons). The energy can be of various forms, from heat, microwave, to electricity and light (ultraviolet light or intense visible light from a laser), among which electricity is the most commonly used form of energy. Currently, different types of microfluidic plasmas have been developed, with the application fields ranging from chemical analysis, nanomaterials synthesis to surface modification.

A salient configuration is “microfluidic chip-factory” **(Figure 8)**, as reported by Li et al [65]. A microfluidic plasma chip which consists of reaction zone, gas-liquid separator, collection and UV-Vis detection chamber together for the synthesis of gold nanoparticles and their on-site detection of mercury ions. HAuCl4 solution was injected into the reaction zone and being reduced to gold nanoparticles under the helium plasma treatment. Afterwards, the gas and liquid phases of the segments were separated by a downstream micro chamber. Due to surface tension and the density difference between the liquid and gas, the liquid part was captured by the lower chamber, while the gas part was extracted by the upper chamber. The collected gold nanoparticles were then injected into the collection chamber for UV-Vis detection of mercury ions. It is shown “reaction-separation-detection” can be integrated into a single chip to form a microfluidic plasma based “chip-factory”, and the detection limit of Hg2+ concentration was found to be 10-6 M.

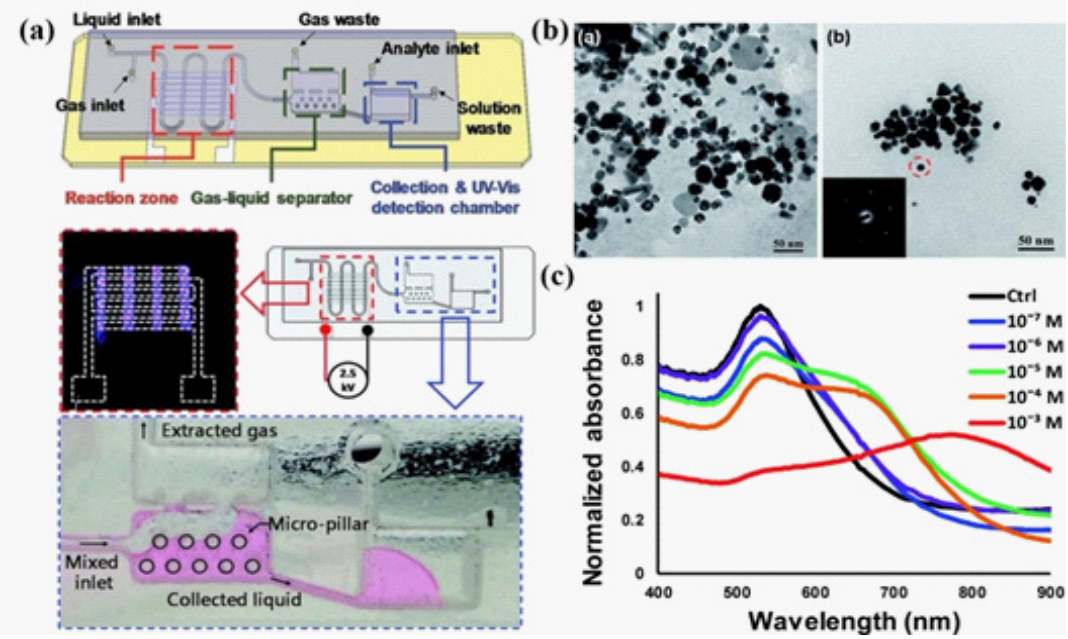

Figure 8: (a) Illustration of the microfluidic plasma based "chip-factory" for the synthesis of Au nanoparticles and the detection of Hg2+; (b) TEM images of the synthesized Au nanoparticles; (c) UV-Vis absorbance spectra for detecting mercury ions at different Hg2+ concentrations.

3. Characterization techniques related to microplasma-based nanofabrication

3.1. Diagnostics of microplasmas

The simplest and most convenient way to characterize the microplasma is via the visual observation. The atomic and molecular electronically excited states formed in the discharges will emit light during radiative relaxation process. Meanwhile, since different species have their specific excited states and emit lights of different colors (wavelengths), the visual appearance of plasma can already provide direct and useful information about the radical states existing in the plasma. Moreover, the dynamic development of microplasma can be studied by high-resolution photography in time and space. In a microfluidic plasma study, Zhang et al. [66] used a charge-coupled device (CCD) camera for the observation of flow dynamics in a plasma/liquid microreactor, and images of plasma discharge inside the reactor were captured by an intensified charge-coupled device (ICCD) camera. This was triggered by an external function generator and the gate delay and width are 999 μs and 2 μs respectively. Results are shown in **(Figure 9) (a-b)**, and the plasma discharge can be observed in the cavity structure and the discharge is inhomogeneous in different cavities. Another study conducted by Kim et al observed the development of plasma within the microchannel, in which CCD images clearly indicate each stage of plasma development, including ignition, expansion and stable state **(Figure 9(c-f))** [67].

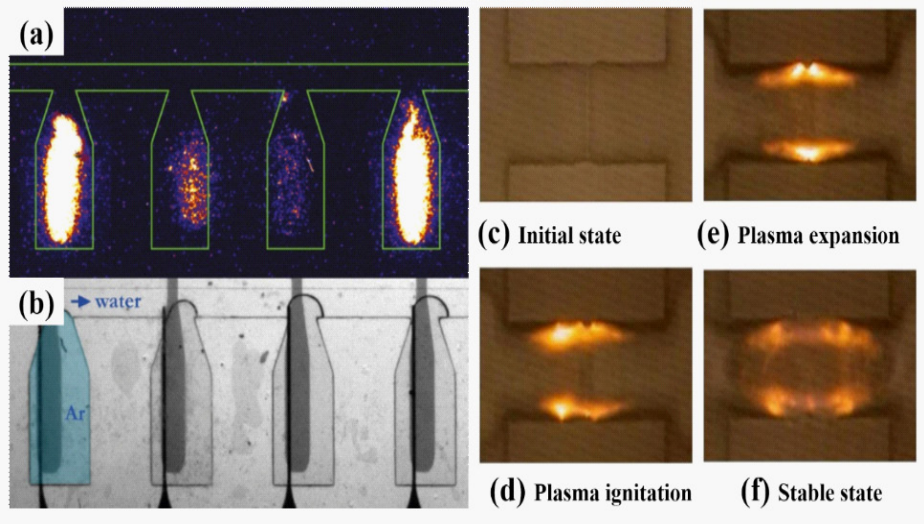

Figure 9: (a) CCD images of plasma discharge in gas liquid flow; (b) CCD image of gas/liquid flow; (c-f) CCD images taken during microplasma generation in a sealed microfluidic glass chip using a water electrode.

Electrical measurement mainly includes the measurement of voltage and current in the working process and the calculation of output power. It is necessary to monitor and control all plasma-generated discharges. In different types of discharge, DBD is one of the most studied plasma discharge, because it is easy to be generated in the microfluidic channel. For this type of microfluidic plasma, the electrical characterization follows the general principle of plasma, and more details have been explained in reference [68]. Voltage and current probes (or current transformers) are often used to measure electrical parameters. It should be noted that the current probe is usually connected between the reactor and the ground to avoid the possible influence of partial discharge current outside the reactor.

Optical emission spectroscopy (OES) is another important technique for microfluidic plasma diagnosis. Because of its simplicity and non-invasiveness, OES has been widely used in many different types of plasma discharge studies. The emission spectrum provides important information about the substances produced under the condition of plasma, which can be further used to analyze the reaction conditions and mechanism. Ishii et al. studied the effect of different gas composition on the emission spectrum of plasma produced in adamantane microfluidic plasma reactor by detecting the CH $A2\Delta \rightarrow X2\Pi$ band at 431.3 nm and the Hα band at 656.3nm [69]. The results are shown in Fig. 10, where both the CH band and the Hα line appeared when H2 was added to the mixture. By comparing with their previous study [70], the authors conclude that less energy is required to dissociate adamantane in the presence of high concentration of H2.

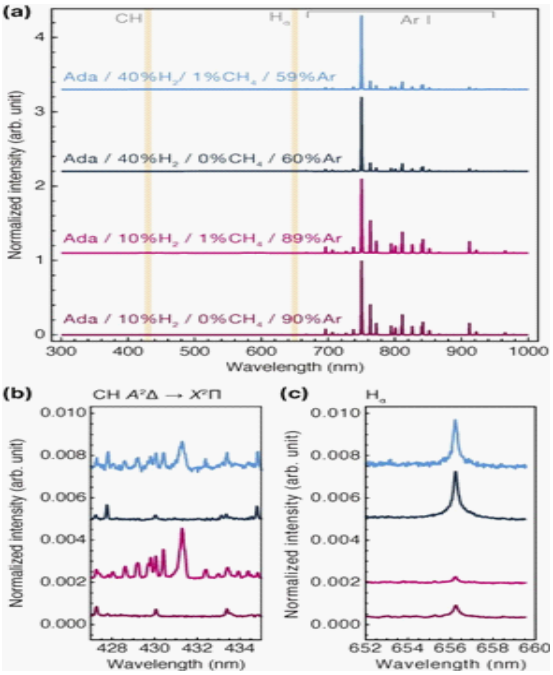

Figure 10: Emission spectra of plasma generated in a microfluidic reactor with different gas composition. (a) Spectra for the four different plasma gas mixtures between 300 and 1000 nm. The two vertical lines represent the locations of the CH band and the Hα line. (b) CH A2 Δ → X2Π band at 431.4 nm. (c) Hα line at 656.3 nm.

In addition, OES can also be used to study plasma parameters. Toshiki et al. reported their research on the generation of spark discharge in microchannels and estimated the electron excitation temperature (about 2.1 × 104 K) based on the Boltzmann diagrams of He and Ar line s[71]. In principle, there is no significant difference in optical diagnosis between microfluidic plasma and bulk plasma. The general method and technique are the same. For example, the spectrum of the N2-second positive system can be inferred from the SPECAIR model (a program for calculating, manipulating and fitting the spectrum) [72], the electron density can be measured by the Stark broadening of the hydrogen Balmer-β line at 486.1 nm, and the electron temperature can be measured by the line ratio technique [73, 74].

As a passive diagnostic method, OES only acquires the information of the emitted material in the plasma. Laser-based techniques are also useful, although surface scattering can sometimes cause problems [75]. Different types of laser-based techniques have been developed for plasma diagnostics, including laser-induced fluorescence (LIF), scattering, absorption and interferometry. Dilecce et al. believe that LIF is a very good instantaneous species measurement technique, which has a good combination of sensitivity, temporal and spatial resolution [76]. In addition to LIF, scattering technique is also very helpful for the diagnosis of microfluidic plasma. For example, Rayleigh scattering and Raman scattering can determine the gas temperature and rotation temperature of molecular species, respectively, and Thomson scattering can determine the electron temperature and electron density in the plasma [77]. Laser interferometry can also be used to measure the numerical density of electrons and gases in small-size plasmas. In some studies, this technique has been applied to the diagnosis of microplasmas [78, 79].

Time-resolved plasma characterization technology allows detailed diagnosis of transient plasma. In the study of Yu et al., time-resolved laser-induced breakdown spectroscopy (LIBS) is usually used to study the characteristics of plasma [80]. The experimental data are processed by classical programs based on Stark effect, Boltzmann and Saha-Boltzmann diagram methods. It is found that the electron density and temperature in the plasma are functions of its decay time. Therefore, comparing the time evolution of the signal-to-noise ratio, time-resolved LIBS technique can measure the relative concentration of ultra-trace elements relative to the reference elements.

The development of diagnostic technology enables us to have an in-depth understanding of complex plasma processes and provide valuable information for the effective development of plasma kinetic models. In order to guide researchers in this field, plasma characterization techniques are summarized in **(Table 4)** [81].

Table 4: Overview of the plasma diagnostic methods. Reprinted with permission from [81]. Copyright 2016 IOP Publishing.

Quantity	Method	Comment
I, V	Shunt resistor, Rogowski coil, voltage dividers	
P	(a) Current-voltage (b) Voltage-charge (c) Thermally based power meters	(a) Used for pulsed, DC and AC discharges (b) Typically used for DBD (c) Used for RF and MW discharges
n_e	(a) Stark broadening (b) Thomson scattering (c) Interferometry (d) Continuum radiation	(a) Typically H_β, $n_e > 10^{20}$ m^{-3} (b) *In situ*, calibration necessary (c) Line of sight measurement, effect of T_g (d) Absolute calibration necessary
T_e	(a) Thomson scattering (b) Line intensity ratio rates only available for limited gas mixtures (c) Continuum radiation	(a) In situ (electron energy distribution function (EEDF) remains a challenge) (b) Need of collisional radiative model, reaction (c) Absolute calibration necessary
T_g	(a) Rotational emission spectra (b) Rotational absorption spectroscopy (c) Rotational LIF spectra (d) Rotational Raman Scattering (e) van der Waals broadening (f) Doppler broadening (g) Rayleigh scattering (h) Schlieren imaging	(a) Non-equilibrium effects possible (b) Ground state diatomic molecule (c) Ground state diatomic molecule (d) Ground state diatomic molecule (e) Atomic line with small Stark broadening at low gas temperatures (f) Atomic line with small Stark broadening at elevated gas temperatures (g) Gas density measurement, species dependent (h) Refractive index measurement
E/N	(a) $N_2(C)$ /$N_2^+(B)$ ratio (b) Coherent anti-Stokes Raman scattering (CARS)	(a) Electron excitation should be dominant (b) Performed in H_2 and N_2 containing gases
H_2O	(a) Absorption (b) Raman scattering (c) OH LIF (quenching measurement)	(a) Line integrated measurement (b) Spatially resolved but less sensitive (c) Other gas molecules determine detection limit

N_2,O_2	(a) Raman scattering (b) Mass spectrometry	(a) Spatially resolved (b) Sampling only at solid interface
O•, N•, H•, …	(a) TaLIF (b) Vacuum ultraviolet (VUV) absorption (c) Mass spectrometry	(a) Requires calibration and quenching corrections (b) Requires VUV wavelengths which are absorbed in O_2, H_2O (c) Sampling only at solid interface, interferes with cracking patterns from internal MS ionization source
•NO, •OH,	(a) LIF (b) UV absorption (c) Mass spectrometry	(a) Requires calibration (b) Line integrated measurement (c) Sampling only at solid interface, interferes with cracking patterns from internal MS ionization source
Ar_m, He_m, $N_2(A)$	(a) LIF (b) Diode laser absorption	(a) Requires calibration by eg. Rayleigh scattering (b) Line integrated measurement
(H)$NO_x^{(-)}$, H_2O_2,	Multi-pass absorption (FTIR)	Line integrated measurement
Positive ions	(a) Mass spectrometry (b) LIF	(a) Sampling only at solid interface (b) Only particular ions such as Ar^+, N_2^+have been studied
Negative ions	(a) Mass spectrometry (b) Photo-detachment	(a) Sampling only at solid interface (b) Requires absolute determination of n_e

3.2. Charaterizations of microplasma-generated functional nanomaterials

It is well known that the properties of nanomaterials are closely related to their composition, structure, size and morphology. In order to determine their physical and chemical properties, it is generally necessary to supplement analytical techniques to obtain comprehensive information. The rapid development of characterization methods and techniques enables us to evaluate nanomaterials from different aspects. In this section, we attempt to summarize several important techniques widely used to characterize the preparation of functional nanomaterials by micro-plasma: scanning electron microscope (SEM), transmission electron microscope (TEM), x-ray diffraction (XRD), x-ray photoelectron spectroscopy (XPS), Fourier transform infrared spectroscopy (FT-IR), energy dispersive x-ray spectroscopy (EDS) and Raman spectroscopy.

3.2.1. SEM and TEM

SEM and TEM are considered to be the two most important techniques for characterizing the morphology, size and size distribution of nanomaterials. In the scanning electron microscope analysis, the electron beam scans the sample surface to generate an image, which leads to the release of electrons on the sample surface. These electrons contain information such as the size, shape, texture and composition of the sample, which is then dispersed and detected by a variety of detectors to produce an image. In TEM characterization, the electron beam is not scanned through the surface of the sample, but transmitted through the sample to form an image. In addition, due to the short electron wavelength, TEM analysis has the ability to capture ultra-fine details, such as a row of atoms or even individual nanoparticles, at extremely high magnification. Therefore, it can be used to observe and calculate the lattice fringes and

lattice space of functional nanoparticles, which is helpful to determine their crystal structure.

3.2.2. EDS

EDS is a technique used to analyze the type and content of elements in a selected area. In EDS measurements, the high-energy electron beam focuses on the sample, excites and ejects electrons from the inner layer of the atom. At the same time, the outer electrons spontaneously fill the hole and release energy in the form of x-rays. Because each element has a fixed atomic structure, the x-rays released can be used to indicate the composition of the element. Typically, EDS is done in conjunction with SEM or TEM analysis. In addition to EDX, there are many techniques to study chemical constituents, such as XRF, XPS, ICP-MS, ICP-OES and atomic absorption spectrophotometry. They can provide supplementary information for plasma to generate functional nanomaterials.

Ghosh et al. used microplasma induction technology to form conductive metal patterns in situ. In this study, Ag cations were contained in PAA solution and deposited on Si substrates to form Ag-PAA films. The deposited film was reduced by micro-plasma, and the silver ion was reduced to metal silver pattern. The microplasma reduction lines were characterized by SEM and EDX, and the formation properties of silver nanoparticles were understood. A typical image of Ag mode is shown in **(Figure 11)**. The results show that the metallization of Ag+ occurs in a region of about 5 μm near the surface of the film, where Ag+ is reduced by microplasma electrons to form Ag particles. Cross-sectional analysis and EDX results further confirmed the reduction and formation of Ag particles, and Ag particles were widely confined near the surface of the film.

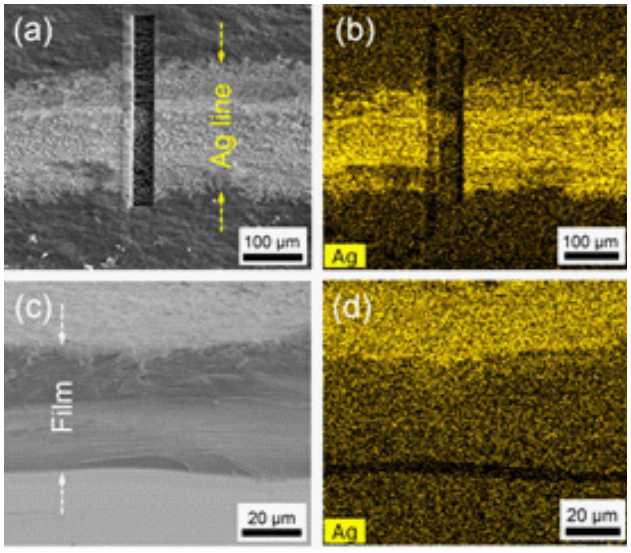

Figure 11: (a-b) Surface and (c-d) cross-sectional SEM and EDX images of the Ag metal patterns fabricated by a microplasma-reduced approach.

3.2.3. XRD

XRD is a popular instrument, which uses X-ray scattering to study the composition and structure of materials, and even the arrangement of atoms in crystals. As the most commonly

used technique to distinguish the purity and crystallinity of inorganic materials, it has been widely used to characterize nitride nanomaterials produced by plasma. In order to explore the possibility of preparing TiN nanoparticles by argon microplasma at atmospheric pressure, Lin et al. used TiCl4 and N2 as precursors[82]. The composition and crystal structure of the obtained products were analyzed by X-ray diffraction (XRD). As shown in **(Figure 12)** (a), this technique can generate crystalline TiN nanoparticles directly from N2 at atmospheric pressure. However, due to the high reaction activity of TiCl4, both anatase and rutile TiO2 exist in the product. Further studies show that the addition of H2 in the synthesis process can effectively reduce the content of TiO2. In addition to nanoparticles, XRD can also be used for the characterization of thin films. Khan et al. deposited iron nitride thin films on flexible polymer substrates by magnetron sputtering in Ar/N2 atmosphere [83]. High purity round iron (99.995% Fe content) was used as sputtering target. XRD results show that iron nitride with different composition and structure can be formed by changing the concentration of N2, such as Fe2N0.94, FeN0.095, Fe24N10, FeN0.056, Fe4N and Fe16N2 **(Figure 12 (b))**.

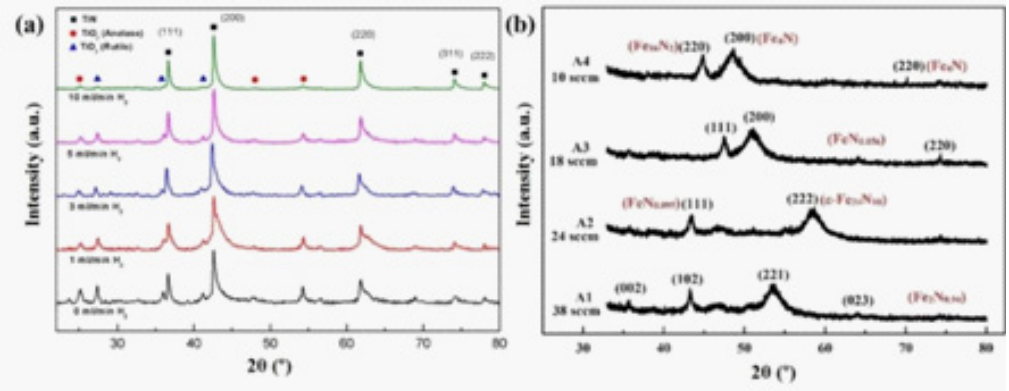

Figure 12: (a) XRD results of the microplasma-generated TiN nanoparticles, with the addition of different H2 concentrations. Reprinted with permission from [82], copyright 2017 Elsevier; (b) XRD patterns of iron nitride films obtained at various N2 gas flow rate using the magnetron sputtering method.

3.2.4. XPS

XPS is a widely used technique to characterize the chemical composition of materials. During the measurement, a beam of x-ray photons is irradiated on the sample, in which the core electrons are ejected from the initial state. By recording electrons ejected within a certain range of electron energy, it can identify and quantify all existing elements. In addition, it has the ability to understand the atomic chemical state and bonding information, which makes it have application potential in many fields.

Compared with EDX characterization, one of the unique advantages of XPS is that it can obtain the chemical state information of atoms (such as the oxidation state of elements), which has practical significance in many fields. However, due to the limited depth of electron escape, XPS can only detect the signal of < 10 nm sample depth. Therefore, it is considered as a surface characterization technique instead of bulk material analysis. In addition, in order to achieve sufficient chemical specificity and spatial resolution, ultra-high vacuum is needed

in the measurement process of XPS (P < 100.9 millibar). In this thesis, the complementary information of the prepared nanoparticles was analyzed by electron spectroscopy (EDX) and x-ray spectroscopy (XPS).

3.2.5. FT-IR

FT-IR spectroscopy is an analytical tool to identify organic, inorganic and, in some cases, polymer materials. In the process of measurement, the test sample will produce molecular vibration and produce the absorption spectrum in the mid-infrared range. The spectrum provides information about the chemical bonds and molecular structure of the sample and can be used to determine how molecules combine on the surface or as part of the sample. Because of its fast, economical and non-destructive properties, FT-IR has become an important tool for in-situ and non-in-situ characterization of materials, and has been widely used in the analysis of functional nanomaterials produced by microplasma.

3.2.6. Raman spectroscopy

Raman spectroscopy is a spectral tool discovered by Indian scientist Chandrasekhara Venkata Raman based on inelastic scattering effect. Laser is generally used as the light source of monochromatic light. When the photon in the monochromatic light is absorbed by the sample, its frequency moves up and down relative to the original monochromatic light frequency, which provides information about low-frequency transitions such as molecular rotation and vibration [84].

(Table 5) summarizes the advantages and disadvantages of the above techniques. There are other characterization methods for the preparation of functional nanomaterials by plasma, such as x-ray fluorescence (XRF), BET, atomic force microscope (AFM), selective region electron diffraction (SAED), inductively coupled plasma mass spectrometry (ICP-MS) and so on. It should be noted that in order to obtain comprehensive and accurate product information, samples need to be tested with a variety of characterization tools. Before being applied to specific applications, it is necessary to have a comprehensive understanding of their physical and chemical properties.

Table 5: Pros and cons of typical characterization methods for the microplasma-generated functional nanomaterials.

Tool	Advantages	Drawbacks
SEM	High resolution; wide range of magnification; good comparative information; ability to image complex shapes	Expensive and large; may destructive; may require sputter coating; limited to solid samples
TEM	High resolution; high information content; wide range of magnification	Expensive; high vacuum; strict working condition
XRD	Allowing liquid and gas phase analysis; non-destructive; no sample preparation needed	Not suitable for amorphous samples; no quantitative analysis
XPS	Nondestructive; surface sensitive; quantitative; chemical bonding information; less interference	Expensive; large analysis area; high vacuum; low resolution; slow
EDS	Fast analysis; high sensitivity; good repeatability	Low energy resolution; low peak to background ratio; limited quantification
FT-IR	Sensitive; fast; easy; relatively inexpensive; powerful data station; in-situ and ex-situ analysis	Cannot detect atoms, monoatomic ions, molecules containing two identical atoms
Raman	Non-destructive; no pretreatments; no specific sample preparation needed; fast analysis; high sensitivity	Interference of fluorescence from the optical system or the environment

4. Salient Examples of Microplasma-Assisted Nanomaterials Synthesis

At present, the preparation of nanomaterials is considered to be one of the most promising research fields. Microplasma is especially suitable for the preparation of nanomaterials because of its unique characteristics, such as non-equilibrium state, stable operation at atmospheric pressure and room temperature, high free radical density and so on. It can effectively dissociate precursors and nucleate nanoparticles at the atomic level, allowing the preparation of nanoparticles with a particle size of less than 10 nm through the so-called "bottom-up" method. In recent years, with the synthesis of nanomaterials, micro-plasma devices with different configurations have been developed.

4.1. Metal nanoparticles

Metal nanoparticles, particularly noble metal nanoparticles, show promising prospects in cancer treatment due to their unique characteristics such as high surface to volume ratio, facile surface chemistry, excellent optical properties as well as the ability to convert radio frequencies or light into heat. For instance, they can extravasate into tumor stroma and accumulate at tumor sites, and be tracked directly by optical microscopy because of their special optical and imaging properties. Furthermore, noble metal nanoparticles hold great promise to kill cancer cells selectively through hyperthermia effect. The existence of high-density and high-energy electrons in microplasma makes it possible for the decomposition of precursors and the in-situ nucleation of nanoparticles. As mentioned in the previous section, Chiang et al. [85] synthesized iron and nickel nanoparticles from ferrocene and nickel respectively through a hollow electrode microplasma system. Compared with other methods, the prepared nanoparticles have narrow dispersion and non-aggregation. Bimetallic and polymetallic

nanoparticles, such as NixFe1-x[86], Ni0.47Cu0.53, Ni0.18Cu0.82, Ni0.22Fe0.29Cu0.49 and Ni0.34Fe0.46Cu0.20, were also synthesized in microplasma systems [24].

The innovative idea of combining non-thermal plasmas and microfluidics offer a new pathway to prepare functional nanomaterials continuously and controllably. For examples, in the study of Mariotti et al., a non-thermal plasma jet confined within a quartz capillary is applied for the gas-phase synthesis of Sn nanocrystals **(Figure 13)**. Helium is selected as the plasma gas, and the gas flow rate is adjusted in the 0.25-1 SLM range to control the residence time of the precursors. By regulating the operational parameters such as the gas flow rate, gas composition and plasma power, their effects on the products are investigated. Surfactant-free, ultrasmall, free-standing Sn nanocrystals of high crystallinity and purity are synthesized by the capillary-confined plasma jet. Moreover, the designed microfluidic plasma allows accurate control on the size, morphology and crystal structures of the products by tuning operational parameters. Due to the microreactor geometry, the reaction volume is on the order of nanolitres. Meanwhile, with flow rates in the 0.25-1 sLm range, the residence times of the precursor is estimated to be ~1 μs, and can be easily adjusted via mass flow controller. In the lowest flow rate (0.25 sLm), tetragonal structure (β-phase) Sn nanocrystals with a mean diameter of 6.07 nm are formed. Increasing the flow rate leads to a phase transition from tetragonal phase to diamond phase (α-phase), and mixed α-/β-phase Sn particles with progressively smaller diameters (2-3 nm) are observed in the 0.5-0.75 sLm range.

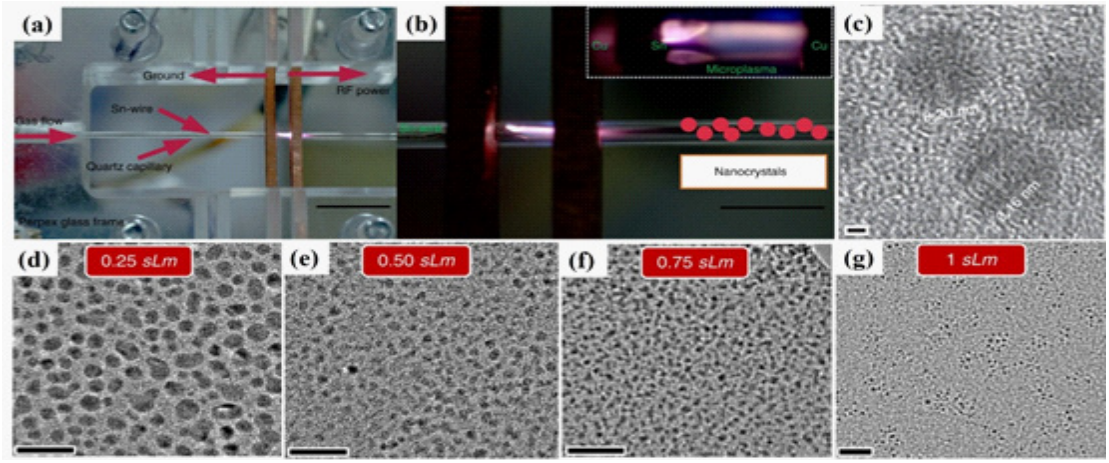

Figure 13: (a) Microfluidic plasma reactor for the synthesis of Sn nanoparticles; (b) A high-resolution photograph of the plasma confined within a quartz tube, showing clearly the plasma region; (c) A High-resolution transmission electron micrographs of the obtained Sn nanoparticles, suggesting their crystal structure; (d-g) TEM images of Sn nanocrystals prepared at various gas flow rates (from 0.25 SLM to 1 SLM).

4.2. Si nanomaterials

As one of the most abundant elements on earth, Si is famous for its applications in the semiconductor industry. However, the indirect band gap of silicon will lead to poor optical properties, which limits its application in some fields. In recent years, nanostructured Si has aroused great interest because of its good stability and non-toxicity, and has become one of the most popular functional materials in the electronic industry. They have been produced by

different microplasma configurations by using silicon tetrachloride (SiCl4) or silane (SiH4) as precursors. In the unique plasma media, the agglomeration of nanocrystals is inhibited, and small nanocrystals are recombined through unconventional heating ions of electron beam and other processes that may lead to the crystallization of small particles. For example, Askari used a RF microplasma jet for the synthesis of Si NPs. Results showed they are extremely small (2~4 nm), have spherical morphology, excellent crystallinity, and no agglomeration [87]. In addition, owing to the effective heating in non-thermal microplasma, it is proved that Si NPs can nucleate and grow at a temperature much lower than its crystallization threshold. Another example for the synthesis of Si NPs is demonstrated by Mangolini, in which SiH4 is used as the precursor and Ar as carrier gas. High quality Si nanoparticles with blue luminescent and a yield of 1452mg/h were prepared by hollow electrode microdischarge. The size of Si NPs was measured to be in the range of 1~3 nm [88, 89]. Moreover, the admixture of H2 in the plasma lead to surface passivation of Si, resulting in decreased possibility of Si condensation and particle growth rate.

4.3. Metal-oxide nanomaterials

Doe to their unique mechanical and chemical properties, metal oxide nanostructures have the potential to play important roles in many technologies, such as sensing devices [90], biomedical applications [91], energy saving [92], catalysis [93], wastewater treatment [94] and so on. At present, various microplasma configurations and processes have been developed for the production of metal oxide nanomaterials. The most commonly adopted configuration is microplasma jet, for it allows various ways to couple the electrical energy to ignite and maintain the plasma. Besides, it is also convenient to use sacrificial metal electrodes as precursors, or tubes/external electrodes with flexible precursors.

In the study of Lin et al, iron oxides NPs were prepared from ferrocene by a hollow-cathode DC-driven microplasma to show the feasibility and unique advantages of the plasma nanofabrication technique. It is shown small nanoparticles of 8-15 nm were continuously synthesized. Meanwhile, the control over particle size can be achieved by adjusting the precursor concentration or the plasma power. The reported method can be extend to the preparation of a series of oxide NPs like CuO, PdO and NiO by choosing organometallic precursors such as Cu(hfac)2, Pd(hfac)2, or nickelocene, respectively. In addition to the gas-phase nanofabrication, metal oxide NPs can also be prepared through liquid-phase plasma process. For instance, Cu2O and Fe3O4 NPs have been prepared by GDE method. Compared with the micro-plasma jet, the liquid-phase micro-plasma is much easier to set up, because all the nanoparticles can be collected in the solution, not in the matrix. In addition, it does not need to provide O2 as a precursor because O• can be obtained from H2O.

4.4. Carbon nanomaterials

Carbon nanomaterials have aroused great interest in many potential application fields because of their excellent properties. For example, nano-diamond has excellent hardness, high thermal conductivity and chemical stability, so it is used as an excellent filling material composite material [95]. With the addition of nano-diamond, the mechanical strength, thermal conductivity, adhesion and wear resistance of the polymer can be significantly improved. In addition, they are non-toxic, good biocompatibility and adjustable surface chemical properties, so they are especially suitable for biomaterials used in bone tissue engineering [96]. In recent years, a series of carbon nanomaterials have been prepared by microplasma technology, including carbon nanotubes [32, 85, 97, 98], nano-diamond [25, 99], nanorods [98], carbon nanoparticles [100] and so on. In this section, several typical examples are introduced.

An intelligent microplasma system for producing nano-diamond at atmospheric pressure and room temperature uses a hollow electrode micro-discharge structure [25]. Ethanol vapor was selected as the carbon source, and the microplasma was introduced continuously through the mixture of Ar and H2. A glass filter is installed at the outlet of the aerosol flow to collect nanoparticles. The results show that high purity nano-diamond can be prepared by this method under relatively neutral conditions. In the process of dissociation, the existence of C2 and CH• promotes the nucleation of solid carbon clusters and nano-diamond respectively, but the specific mechanism has not been discussed. The introduction of H2 affects the growth of diamond and the etching of non-diamond carbon, which leads to the stability of diamond phase carbon and the selective removal of non-diamond phase carbon. Another example of nano-diamond crystal deposition is achieved through a microplasma array [99], in which four jets run parallel in the capillary. The device uses H2 and CH4 as precursors and deposits at subatmospheric pressure (200 Torr). Molybdenum foil was used as substrate and insulated at 800 ℃. The results show that high quality diamond nanocrystals can be prepared at different CH4 concentrations [92].

4.5. Nitride nanomaterials

Nitride nanomaterials have been widely applied in the fields of optics, thermal insulation coatings, biomedical equipment, semiconductors and strengthening and toughening materials. For example, ScN and its alloy Al1-xScxN are considered to be attractive energy transfer and conversion materials. CrN is expected to have a great application prospect in thermoelectric applications. Rare earth nitrides such as YN, GdN and ErN exhibit strong magnetic properties in contrast to the spin and orbital moment coupling in the 4f shell, which can be used in optoelectronic and spintronic applications. However, nitrogen molecules are quite inert because of their triple bonds and very stable electronic configurations. They cannot be directly consumed or converted into organic compounds by animals. Due to the high reactivity of plasmas, an emerging research field lies in the application of microplasma technique for the

preparation of N-containing nanomaterials.

Some studies have directly prepared nitrogen nitride nanomaterials (such as BN, TiN, GaN, Si3N4) using N2 or NH3 as nitrogen sources, while some researchers have shown great interest in the preparation of carbonitride, oxynitride or oxocarbon nitride nanomaterials. For instance, Knoops et al. developed a plasma-based atomic layer deposition process for the preparation of high quality Si3N4 films, where Bis(t-butylamino)silane ([NH(C4H9)]2SiH2) was transported by argon into a N2 plasma to form the target product. The demonstrated method indicated silicon nitrides could be formed by using N2 as the N source at significantly lower temperatures (from room temperature to 200 °C). In the study of Haye et al., ε-Fe3N-type nanoparticles were fabricated in a nitrogen-containing RF microplasma discharge. Iron acetylacetonate [Fe(acac)3] and ammonia were selected as the iron and nitrogen source. Owing to the high reactivity of plasma, Fe(acac)3 was degraded to form iron nanoparticles. Meanwhile, NH3 was also activated and being decomposed to form nitrogen species, resulting in the direct generation of Fe3N nanoparticles on carbon support.

4.6. Polymer nanomaterials

Plasma polymerization is a process in which organic and inorganic polymers are deposited from a monomer vapor by the use of an electron beam, ultraviolet radiation, or glow discharge. It provides the deposition of nanocoatings on fibers via gas phase activation and plasma substrate interactions. This environment-friendly durable nanocoating method overweighs conventional coating methods as it needs a very low material and energy input, without interference to the bulk properties of textiles such as feel, handle, optical properties, and mechanical strength. Over the past years, deposition of thin flexible films was considered as one of the most promising applications for the plasma technology. These layers have been broadly used in various fields, ranging from food, beverage, medical and drug packaging to more demanding purpose, such as organic photovoltaic (OPV) devices, flexible solar cells or LED displays.

Lee and Shim synthesized acrylic acid-grafted pH-responsive poly(vinyledene fluoride) (PVDF) membranes using a plasma polymerization method. The results revealed that the degree of grafting depends on the plasma exposure time. Also, the pH responsiveness analyzed with riboflavin flux showed that the permeability of riboflavin decreased drastically in between pH 4 and 5. Based on this finding, they further prepared pH and temperature dual-responsive membranes using the same procedure. Starostin et al., demonstrated a DBD-based roll-to-roll PECVD reactor for the deposition of silicon oxycarbonitride film. In this study, the DBD plasma was sustained between two cylindrical rotary drum electrodes, and being equipped with roll-to-roll foil transport and tension control system. The effective discharge width and the smallest gap distance was 15 cm and 0.5 mm, respectively. The electrodes surface was covered by a polyethylene-2,6-naphthalate (PEN) foil, which not only served as the deposition

substrate but also as the dielectric layer in the DBD arrangement. Tetraethylorthosilicate, Si(OC2H5)4, was used as the starting material and carried into the plasma zone by a N2 gas flow (20 slm). Meanwhile, O2 was used as the reactive gas. Due to the high reactivity of the plasma, precursors were immediately dissociated when they were introduced into the plasma zone. Results showed uniform, smooth and well adherent silicon oxycarbonitride coatings were continuously deposited on the PEN foil in an atmospheric pressure process. Moreover, the chemical composition, morphology and moisture barrier performance of the deposited coating were found as a function of the dynamic deposition rate and substrate temperature.

The above cases show that the microplasma technnique has a wide range of versatility in the preparation of different kinds of materials, including metals, metal alloys, silicon derivatives, oxides, carbonates, nitrides, polymer nanomaterials, etc. These results also reflect the high flexibility of microplasma configurations and operating parameters.

5. Conclusions

In this book chapter, the recent progress in the preparation of functional nanoparticles assisted by microplasma is reviewed. Firstly, a general overview on nanomaterials, plasma technology, plasma nanofabrication, microplasma and its characteristics is presented. Afterwards, typical microplasma systems for nanomaterials synthesis were discussed, including gas-phase systems, liquid-involved systems and microfluidic plasmas. Meanwhile, representative configurations in each system are demonstrated to show their pros and cons. This is followed by the introduction of the main instrumentation techniques for the characterization of the microplasma as well as the obtained nanomaterials. Finally, a broad category of nanomaterials prepared by microplasmas are presented, such as metal NPs and metal alloys, Si nanomaterials, metal-oxide nanomaterials, carbon nanomaterials, nitride nanomaterials, and polymer nanomaterials.

Microplasma-assisted technology makes great use of the synergistic advantages of microreactor and non-thermal plasma chemistry and provides a simple and innovative route for the synthesis of functional nanoparticles in gas-phase or aqueous-phase. Compared with ordinary wet chemical methods, reducing agents, solvents and stabilizers are no longer needed. As a result, potential side effects and by-products have been greatly reduced, avoiding the use of complex procedures such as separation, centrifugation and washing to obtain high-purity products. In addition, the limitation of microplasma on the micro-spatial scale not only makes the precursor have a high energy density, but also ensures a relatively short residence time and uniform RTD. Therefore, the functional nanoparticles with smaller size and narrower size distribution can be prepared under the plasma dissipation power as low as ~1.0 W, which could not be achieved by the existing methods. Another unique advantage is that the "in-flight" characteristics of functional nanoparticles can be adjusted by simply adjusting the processing conditions. It is expected that this technology can be applied as a "dry process" to

the local production of clearly defined nanostructures (similar to printing technology). With the development of microplasma technology, it is expected that the fabrication of functional nanomaterials at industrial scale is within reach.

6. Acknowledgements

The authors greatly appreciate the funding support from National Natural Science Foundation of China (22078125, 52004102), Natural Science Foundation of Jiangsu Province (BK20190605), Postdoctoral Science Foundation of China (2021M690068), Fundamental Research Funds for the Central Universities (JUSRP221018), and Key Laboratory of Nanodevices of Jiangsu Province (21SZ02).

7. **Notes**

This book chapter is organized based on our previous publications as well as literatures from this field. The main reference are listed below:

1. Microplasma: a new generation of technology for functional nanomaterial synthesis, Plasma Chemistry and Plasma Processing, 2015, 35 (6), 925-962.

2. Microfluidic plasmas: Novel technique for chemistry and chemical engineering, Chemical Engineering Journal, 2021, 417, 129355.

3. Plasma-assisted nitrogen fixation in nanomaterials: fabrication, characterization, and application, Journal of Physics D: Applied Physics, 2020, 53 (13), 133001.

4. Synthesis of metallic nanoparticles by microplasma, Physical science review, 2018, 3(10).

7. References

1. Bai J, Zhou B X. Titanium dioxide nanomaterials for sensor applications[J]. Chemical Reviews, 2014, 114 (19): 10131-10176.

2. Popat A, Hartono S B, Stahr F, et al. Mesoporous silica nanoparticles for bioadsorption, enzyme immobilisation, and delivery carriers[J]. Nanoscale, 2011, 3 (7): 2801-2818.

3. Smith B R, Gambhir S S. Nanomaterials for In Vivo Imaging[J]. Chemical Reviews, 2017, 117 (3): 901-986.

4. Theerthagiri J, Salla S, Senthil R A, et al. A review on ZnO nanostructured materials: energy, environmental and biological applications[J]. Nanotechnology, 2019, 30 (39): 392001.

5. Yang X, Yang M X, Pang B, et al. Gold nanomaterials at work in biomedicine[J]. Chemical Reviews, 2015, 115 (19): 10410-10488.

6. Vons V, Creyghton Y, Schmidt-Ott A. Nanoparticle production using atmospheric pressure cold plasma[J]. Journal of Nanoparticle Research, 2006, 8 (5): 721-728.

7. Kortshagen U R, Sankaran R M, Pereira R N, et al. Nonthermal plasma synthesis of nanocrystals: fundamental principles, materials, and applications[J]. Chemical Reviews, 2016, 116 (18): 11061-11127.

8. Lin L, Wang Q. Microplasma: a new generation of technology for functional nanomaterial synthesis[J]. Plasma Chemistry and Plasma Processing, 2015, 35 (6): 925-962.

9. Mollah M Y A, Schennach R, Patscheider J, et al. Plasma chemistry as a tool for green chemistry, environmental analysis and waste management[J]. Journal of Hazardous Materials, 2000, 79 (3): 301-320.

10. Belmonte T, Arnoult G, Henrion G, et al. Nanoscience with non-equilibrium plasmas at atmospheric pressure[J]. Journal of Physics D-Applied Physics, 2011, 44 (36): 363001.

11. Mariotti D, Ostrikov K. Tailoring microplasma nanofabrication: from nanostructures to nanoarchitectures[J]. Journal of Physics D-Applied Physics, 2009, 42 (9): 1-4.

12. Olabanji O T, Bradley J W. The development and analysis of plasma microfluidic devices[J]. Surface & Coatings Technology, 2011, 205: S516-S519.

13. Stoffels E, Flikweert A J, Stoffels W W, et al. Plasma needle: a non-destructive atmospheric plasma source for fine surface treatment of (bio)materials[J]. Plasma Sources Science & Technology, 2002, 11 (4): 383-388.

14. Hrycak B, Jasinski M, Mizeraczyk J. Spectroscopic investigations of microwave microplasmas in various gases at atmospheric pressure[J]. European Physical Journal D, 2010, 60 (3): 609-619.

15. Sladek R E J, Stoffels E, Walraven R, et al. Plasma treatment of dental cavities: A feasibility study[J]. Ieee Transactions on Plasma Science, 2004, 32 (4): 1540-1543.

16. Kieft I E, van der Laan E P, Stoffels E. Electrical and optical characterization of the plasma needle[J]. New Journal of Physics, 2004, 6: 149.

17. Yanguas-Gil A, Focke K, Benedikt J, et al. Optical and electrical characterization of an atmospheric pressure microplasma jet for Ar/CH4 and Ar/C2H2 mixtures[J]. Journal of Applied Physics, 2007, 101 (10): 103307(1-8).

18. Ichiki T, Taura R, Horiike Y. Localized and ultrahigh-rate etching of silicon wafers using atmospheric-pressure microplasma jets[J]. Journal of Applied Physics, 2004, 95 (1): 35-39.

19. Kono A, Wang J, Aramaki M. Production and characterization of high-pressure microwave glow discharge in a microgap aiming at VUV light source[J]. Thin Solid Films, 2006, 506: 444-448.

20. Hyman J. Conference proceeding for 1997 IEEE 24th international conference on plasma sciences[J]. 1997: 19-20.

21. Belostotskiy S G, Khandelwal R, Wang Q, et al. Measurement of electron temperature and density in an argon microdischarge by laser Thomson scattering[J]. Applied Physics Letters, 2008, 92 (22): 221507.

22. Kurt H, Salamov B G. Breakdown phenomenon and electrical process in a microplasma system with InP electrode[J]. Jom, 2020, 72 (2): 651-657.

23. Loveless A M, Garner A L. A universal theory for gas breakdown from microscale to the classical Paschen law[J]. Physics of Plasmas, 2017, 24 (11): 1-15.

24. Lin P A, Sankaran R M. Plasma-assisted dissociation of organometallic vapors for continuous, gas-phase preparation of multimetallic nanoparticles[J]. Angewandte Chemie-International Edition, 2011, 50 (46): 10953-10956.

25. Kumar A, Lin P A, Xue A, et al. Formation of nanodiamonds at near-ambient conditions via microplasma dissociation of ethanol vapour[J]. Nature Communications, 2013, 24 (11): 1-15.

26. Shimizu Y, Sasaki T, Bose A C, et al. Development of wire spraying for direct micro-patterning via an atmospheric-pressure UHF inductively coupled microplasma jet[J]. Surface & Coatings Technology, 2006, 200 (14-15): 4251-4256.

27. Shimizu Y, Bose A C, Mariotti D, et al. Reactive evaporation of metal wire and microdeposition of metal oxide using atmospheric pressure reactive microplasma jet[J]. Japanese Journal of Applied Physics Part 1-Regular Papers Brief Communications & Review Papers, 2006, 45 (10B): 8228-8234.

28. Bose A C, Shimizu Y, Mariotti D, et al. Flow rate effect on the structure and morphology of molybdenum oxide

nanoparticles deposited by atmospheric-pressure microplasma processing[J]. Nanotechnology, 2006, 17 (24): 5976-5982.

29. Mariotti D, Svrcek V, Kim D G. Self-organized nanostructures on atmospheric microplasma exposed surfaces[J]. Applied Physics Letters, 2007, 91 (18): 183111(1-3).

30. Shimizu Y, Kawaguchi K, Sasaki T, et al. Generation of room-temperature atmospheric H2/Ar microplasma jet driven with pulse-modulated ultrahigh frequency and its application to gold nanoparticle preparation[J]. Applied Physics Letters, 2009, 94 (19): 191504(1-3).

31. Mariotti D, Bose A C, Ostrikov K. Atmospheric-microplasma-assisted nanofabrication: metal and metal-oxide nanostructures and nanoarchitectures[J]. Ieee Transactions on Plasma Science, 2009, 37 (6): 1027-1033.

32. Kona S, Kim J H, Harnett C K, et al. Carbon nanotube growth studies using an atmospheric, microplasma reactor[J]. Ieee Transactions on Nanotechnology, 2009, 8 (3): 286-290.

33. Shirai H, Kobayashi T, Hasegawa Y. Synthesis of silicon nanocones using rf microplasma at atmospheric pressure[J]. Applied Physics Letters, 2005, 87 (14): 143112(1-3).

34. Yoshiki H, Mitsui T. TiO2 thin film coating on a capillary inner surface using atmospheric-pressure microplasma[J]. Surface & Coatings Technology, 2008, 202 (22-23): 5266-5270.

35. Koh T L, O'Hara E C, Gordon M J. Microplasma-based synthesis of vertically aligned metal oxide nanostructures[J]. Nanotechnology, 2012, 23 (42): 425603.

36. Ghosh S, Liu T, Bilici M, et al. Atmospheric-pressure dielectric barrier discharge with capillary injection for gas-phase nanoparticle synthesis[J]. Journal of Physics D-Applied Physics, 2015, 48 (31).

37. Lu N, Liu N, Zhang C, et al. CO2 conversion promoted by potassium intercalated g-C3N4 catalyst in DBD plasma system[J]. Chemical Engineering Journal, 2021, 417: 129283.

38. Mariotti D, Sankaran R M. Microplasmas for nanomaterials synthesis[J]. Journal of Physics D-Applied Physics, 2010, 43 (32): 323001.

39. Lu Y, Xu S F, Zhong X X, et al. Characterization of a DC-driven microplasma between a capillary tube and water surface[J]. Epl, 2013, 102 (1): 15002.

40. Akolkar R, Sankaran R M. Charge transfer processes at the interface between plasmas and liquids[J]. Journal of Vacuum Science & Technology A, 2013, 31 (5): 50811.

41. Ghosh S, Bishop B, Morrison I, et al. Generation of a direct-current, atmospheric-pressure microplasma at the surface of a liquid water microjet for continuous plasma-liquid processing[J]. Journal of Vacuum Science & Technology A, 2015, 33 (2): 1.

42. Baba K, Kaneko T, Hatakeyama R. Ion irradiation effects on ionic liquids interfaced with rf discharge plasmas[J]. Applied Physics Letters, 2007, 90 (20): 201501(1-3).

43. Meiss S A, Rohnke M, Kienle L, et al. Employing Plasmas as gaseous electrodes at the free surface of ionic liquids: Deposition of nanocrystalline silver particles[J]. Chemphyschem, 2007, 8 (1): 50-53.

44. Huang X, Li Y, Zhong X. Effect of experimental conditions on size control of Au nanoparticles synthesized by atmospheric microplasma electrochemistry[J]. Nanoscale Research Letters, 2014, 9.

45. Buzzeo M C, Evans R G, Compton R G. Non-haloaluminate room-temperature ionic liquids in electrochemistry - A review[J]. Chemphyschem, 2004, 5 (8): 1106-1120.

46. Zhang J, Bond A M. Practical considerations associated with voltammetric studies in room temperature ionic liquids[J]. Analyst, 2005, 130 (8): 1132-1147.

47. Vennekamp M, Janek J. Control of the surface morphology of solid electrolyte films during field-driven growth in a

reactive plasma[J]. Physical Chemistry Chemical Physics, 2005, 7 (4): 666-677.

48. Lee H, Park S H, Kim S J, et al. Synthesis of tin and tin oxide nanoparticles using liquid phase plasma in an aqueous solution[J]. Microelectronic Engineering, 2014, 126: 153-157.

49. Lee H, Park S H, Jung S C, et al. Preparation of nonaggregated silver nanoparticles by the liquid phase plasma reduction method[J]. Journal of Materials Research, 2013, 28 (8): 1105-1110.

50. Huang X Z, Zhong X X, Lu Y, et al. Plasmonic Ag nanoparticles via environment-benign atmospheric microplasma electrochemistry[J]. Nanotechnology, 2013, 24 (9): 095604.

51. Hadzifejzovic E, Elahi A, Caruana D J. Control of oxidation state of copper in flame deposited films[J]. Thin Solid Films, 2012, 520 (16): 5254-5259.

52. Cserfalvi T, Mezei P. Direct solution analysis by glow-discharge-electrolyte-cathode discharge spectrometry[J]. Journal of Analytical Atomic Spectrometry, 1994, 9 (3): 345-349.

53. Huang X, Li Y, Zhong X. Effect of experimental conditions on size control of Au nanoparticles synthesized by atmospheric microplasma electrochemistry[J]. Nanoscale Research Letters, 2014, 9 (1): 1-7.

54. Wang R, Zuo S, Zhu W, et al. Rapid synthesis of aqueous-phase magnetite nanoparticles by atmospheric pressure non-thermal microplasma and their application in magnetic resonance imaging[J]. Plasma Processes and Polymers, 2014, 11 (5): 448-454.

55. Du C, Xiao M. Cu2O nanoparticles synthesis by microplasma[J]. Scientific Reports, 2014, 4: 7339.

56. Shahbazali E, Hessel V, Noel T, et al. Metallic nanoparticles made in flow and their catalytic applications in organic synthesis[J]. Nanotechnology Reviews, 2014, 3 (1): 65-86.

57. Kulbe N, Hoefft O, Ulbrich A, et al. Plasma electrochemistry in 1-butyl-3-methylimidazolium dicyanamide: copper nanoparticles from CuCl and CuCl2[J]. Plasma Processes and Polymers, 2011, 8 (1): 32-37.

58. Toriyabe Y, Watanabe S, Yatsu S, et al. Controlled formation of metallic nanoballs during plasma electrolysis[J]. Applied Physics Letters, 2007, 91 (4): 041501(1-3).

59. Suryawanshi P L, Gumfekar S P, Bhanvase B A, et al. A review on microreactors: Reactor fabrication, design, and cutting-edge applications[J]. Chemical Engineering Science, 2018, 189 (1): 431-448.

60. Plutschack M B, Pieber B, Gilmore K, et al. The Hitchhiker's Guide to Flow Chemistry(II)[J]. Chemical Reviews, 2017, 117 (18): 11796-11893.

61. Hessel V, Kralisch D, Kockmann N, et al. Novel process windows for enabling, accelerating, and uplifting flow chemistry[J]. Chemsuschem, 2013, 6 (5): 746-789.

62. Ott D, Borukhova S, Hessel V. Life cycle assessment of multi-step rufinamide synthesis - from isolated reactions in batch to continuous microreactor networks[J]. Green Chemistry, 2016, 18 (4): 1096-1116.

63. Liu X, Surblys D, Kawagoe Y, et al. 30 years of microfluidics [J]. Micro and Nano Engineering, 2019, 2: 76-91.

64. Yao X, Zhang Y, Du L, et al. Review of the applications of microreactors[J]. Renewable & Sustainable Energy Reviews, 2015, 47: 519-539.

65. Li D E, Lin C H. Microfluidic chip for droplet-based AuNP synthesis with dielectric barrier discharge plasma and on-chip mercury ion detection[J]. Rsc Advances, 2018, 8 (29): 16139-16145.

66. Zhang M, Ognier S, Touati N, et al. A plasma/liquid microreactor for radical reaction chemistry: An experimental and numerical investigation by EPR spin trapping[J]. Plasma Processes and Polymers, 2018, 15 (6): 1700188.

67. Jo K-W, Kim M-G, Shin S-M, et al. Microplasma generation in a sealed microfluidic glass chip using a water electrode[J]. Applied Physics Letters, 2008, 92 (1): 011503.

68. Brandenburg R. Dielectric barrier discharges: progress on plasma sources and on the understanding of regimes and single filaments[J]. Plasma Sources Science & Technology, 2017, 26 (5): 053001.

69. Ishii C, Stauss S, Kuribara K, et al. Atmospheric pressure synthesis of diamondoids by plasmas generated inside a microfluidic reactor[J]. Diamond and Related Materials, 2015, 59: 40-46.

70. Stauss S, Ishii C, Pai D Z, et al. Diamondoid synthesis in atmospheric pressure adamantane-argon-methane-hydrogen mixtures using a continuous flow plasma microreactor[J]. Plasma Sources Science & Technology, 2014, 23 (3): 1.

71. Yoshiki H, Sasaki T, Mitsui T. Inner-wall modification of a commercial polymeric microfluidic chip using pulsed He/O-2 and Ar/O-2 mu plasmas[J]. Japanese Journal of Applied Physics, 2018, 57 (12): 126202.

72. Lin L, Starostin S A, Ma X, et al. Facile synthesis of lanthanide doped yttria nanophosphors by a simple microplasma-assisted process[J]. Reaction Chemistry & Engineering, 2019, 4 (5): 891-898.

73. Schoenbach K H, Becker K. 20 years of microplasma research: a status report[J]. European Physical Journal D, 2016, 70 (2): 29.

74. Wang S, Lei G, Liu D, et al. Balmer H-alpha, H-beta and H-gamma spectral lines intensities in high-power RF hydrogen plasmas[J]. Plasma Science & Technology, 2014, 16 (3): 219-222.

75. Tachibana K. Current status of microplasma research[J]. IEEJ Transactions on Electrical and Electronic Engineering, 2006, 1 (2): 145-155.

76. Dilecce G. Optical spectroscopy diagnostics of discharges at atmospheric pressure[J]. Plasma Sources Science & Technology, 2014, 23 (1): 015011-015022.

77. Sommers B S, Adams S F. A comparison of gas temperatures measured by ultraviolet laser scattering in atmospheric plasma sources[J]. Journal of Physics D-Applied Physics, 2015, 48 (48): 1.

78. Urabe K, Muneoka H, Stauss S, et al. Development of Near-Infrared Laser Heterodyne Interferometry for Diagnostics of Electron and Gas Number Densities in Microplasmas[J]. Applied Physics Express, 2013, 6 (12): 126101(1-4).

79. Urabe K, Muneoka H, Stauss S, et al. Microscopic heterodyne interferometry for determination of electron density in high-pressure microplasma[J]. Plasma Sources Science & Technology, 2014, 23 (6): 064007.

80. Lei W, Motto-Ros V, Boueri M, et al. Time-resolved characterization of laser-induced plasma from fresh potatoes[J]. Spectrochimica Acta Part B: Atomic Spectroscopy, 2009, 64 (9): 891-898.

81. Bruggeman P J, Kushner M J, Locke B R, et al. Plasma-liquid interactions: a review and roadmap[J]. Plasma Sources Science & Technology, 2016, 25 (5): 053002.

82. Lin L, Starostin S A, Wang Q, et al. An atmospheric pressure microplasma process for continuous synthesis of titanium nitride nanoparticles[J]. Chemical Engineering Journal, 2017, 321: 447-457.

83. Khan W Q, Wang Q, Jin X, et al. Corrosion, optical and magnetic properties of flexible iron nitride nano thin films deposited on polymer substrate[J]. Physica B-Condensed Matter, 2017, 524: 71-80.

84. Lin L, Ma X, Starostin S A, et al. Color-Tunable Eu3+ and Tb3+ Co-Doped Nanophosphors Synthesis by Plasma-Assisted Method[J]. Chemistryselect, 2019, 4 (14): 4278-4286.

85. Chiang W-H, Sankaran R M. Synergistic Effects in Bimetallic Nanoparticles for Low Temperature Carbon Nanotube Growth[J]. Advanced Materials, 2008, 20 (24): 4857-4861.

86. Zhang F M, Shen J, Sun J F. Processing and properties of carbon nanotubes-nano-WC-Co composites[J]. Materials Science and Engineering a-Structural Materials Properties Microstructure and Processing, 2004, 381 (1-2): 86-91.

87. Askari S, Levchenko I, Ostrikov K, et al. Crystalline Si nanoparticles below crystallization threshold: Effects of collisional heating in non-thermal atmospheric-pressure microplasmas[J]. Applied Physics Letters, 2014, 104 (16): 1-5.

88. Sankaran R M, Holunga D, Flagan R C, et al. Synthesis of blue luminescent Si nanoparticles using atmospheric-

pressure microdischarges[J]. Nano Letters, 2005, 5 (3): 537-541.

89. Mangolini L, Thimsen E, Kortshagen U. High-yield plasma synthesis of luminescent silicon nanocrystals[J]. Nano Letters, 2005, 5 (4): 655-659.

90. Li Y, Della Valle F, Simonnet M, et al. High-performance UV detector made of ultra-long ZnO bridging nanowires[J]. Nanotechnology, 2009, 20 (4): 045501(1-5).

91. Liu G, Gao J, Ai H, et al. Applications and potential toxicity of magnetic iron oxide nanoparticles[J]. Small, 2013, 9 (9-10): 1533-1545.

92. Iida C, Sato M, Nakayama M, et al. Electrodeposition of Cu2O Nanopyramids Using an Anodic Aluminum Oxide Template[J]. International Journal of Electrochemical Science, 2011, 6 (10): 4730-4736.

93. Mariotti D, Lindstroem H, Bose A C, et al. Monoclinic beta-MoO3 nanosheets produced by atmospheric microplasma: application to lithium-ion batteries[J]. Nanotechnology, 2008, 19 (49): 495302(1-6).

94. Dhermendra K T, J. B, Prasenjit S. Application of nanoparticles in waste water treatment[J]. World Applied Sciences Journal, 2008, 3 (3): 1818-4952.

95. Mochalin V N, Shenderova O, Ho D, et al. The properties and applications of nanodiamonds[J]. Nature Nanotechnology, 2012, 7 (1): 11-23.

96. Zhang Q, Mochalin V N, Neitzel I, et al. Fluorescent PLLA-nanodiamond composites for bone tissue engineering[J]. Biomaterials, 2011, 32 (1): 87-94.

97. Chiang W-H, Sankaran R M. Microplasma synthesis of metal nanoparticles for gas-phase studies of catalyzed carbon nanotube growth[J]. Applied Physics Letters, 2007, 91 (12): 121503(1-3).

98. Yoshiki H, Okada T, Hirai K, et al. Growth of vertically aligned carbon nanotube bundles using atmospheric-pressure microplasma[J]. Japanese Journal of Applied Physics Part 1-Regular Papers Brief Communications & Review Papers, 2006, 45 (12): 9276-9279.

99. Sankaran R M, Giapis K P. Hollow cathode sustained plasma microjets: Characterization and application to diamond deposition[J]. Journal of Applied Physics, 2002, 92 (5): 2406-2411.

100. Zou Q, Wang M Z, Li Y G, et al. Fabrication of carbon nanomaterials using pulse microplasma in SEM[J]. Plasma Devices and Operations, 2009, 17 (3): 175-180.